

Supplementary Figure 1:

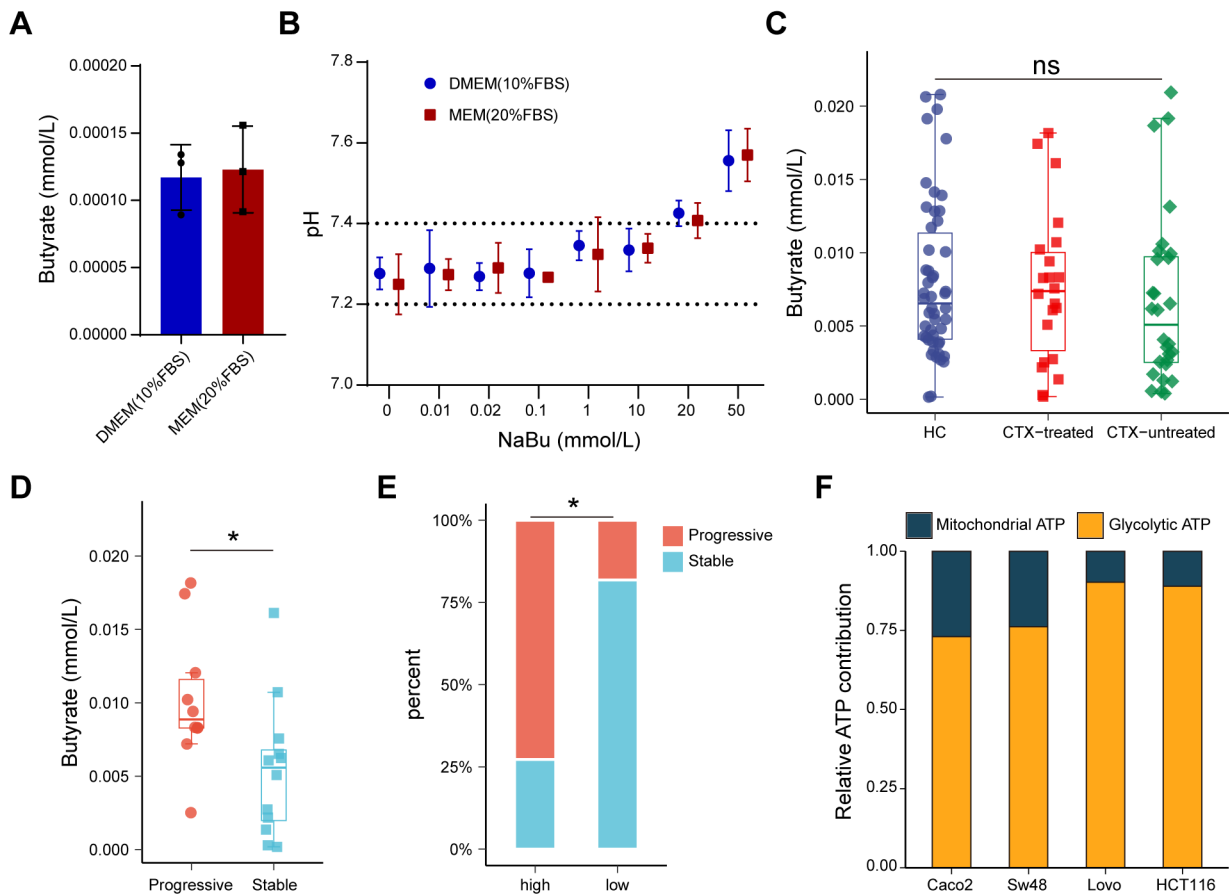


Figure S1. Supplementary analyses of butyrate levels and metabolic background. (A) Background butyrate concentrations measured in different culture media (DMEM with 10% FBS vs MEM with 20% FBS). (B) pH values of culture media after supplementation with the indicated concentrations of NaBu. (C) Circulating butyrate concentrations in healthy controls (HC), CTX-treated CRC patients, and untreated CRC patients (Kruskal–Wallis test). (D) Circulating butyrate levels in CTX-treated CRC patients stratified by response (progressive disease vs stable disease, Wilcoxon test). (E) Proportions of progressive and stable disease in patients with high versus low circulating butyrate levels (Fisher’s exact test). (F) Relative ATP production from glycolysis and mitochondrial oxidative phosphorylation in colorectal cancer cell lines (Caco2, Sw48, LoVo, HCT116). Statistical significance: ns, not significant; * $p < 0.05$.

Supplementary Figure 2:

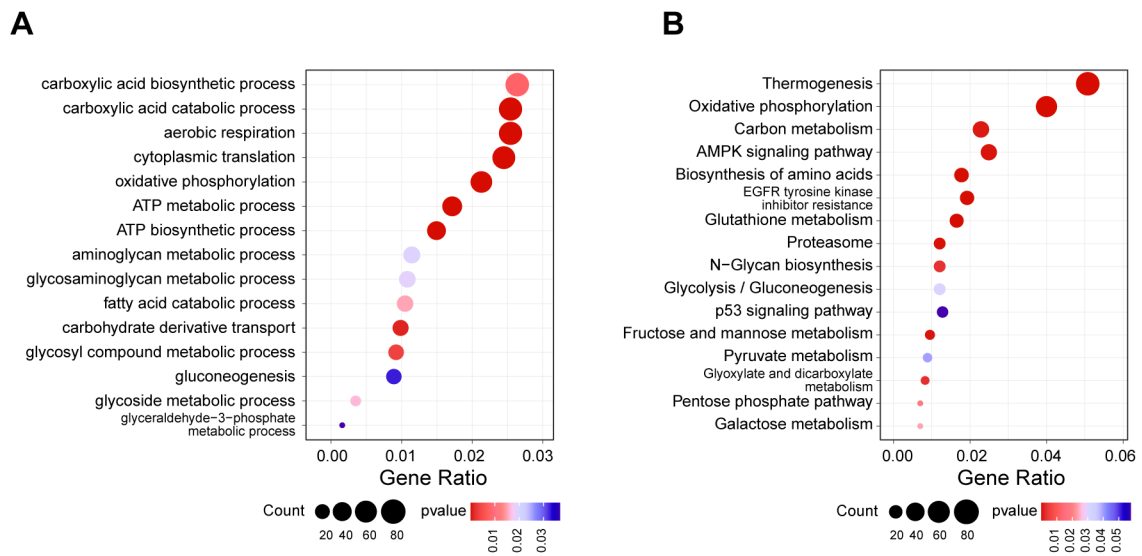
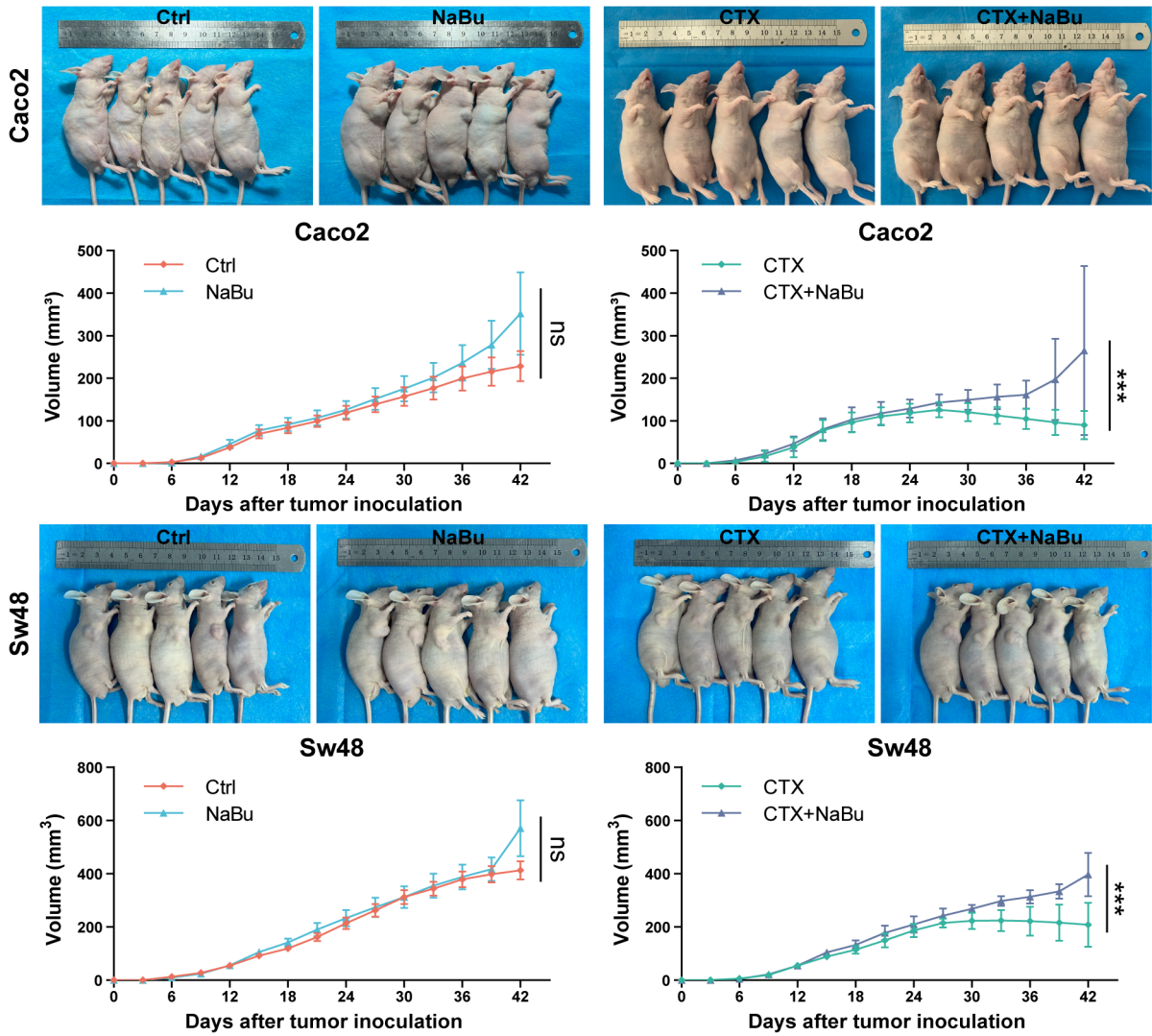


Figure S2. NaBu alters energy metabolism, AMPK, and p53-related pathways in Caco2 cells. (A–B) GO biological process (A) and KEGG pathway (B) enrichment analyses of RNA sequencing comparing CTX+NaBu with CTX alone in Caco2 cells, showing enrichment of energy metabolism, AMPK signaling, and p53-related pathways.

Supplementary Figure 3:

A



B

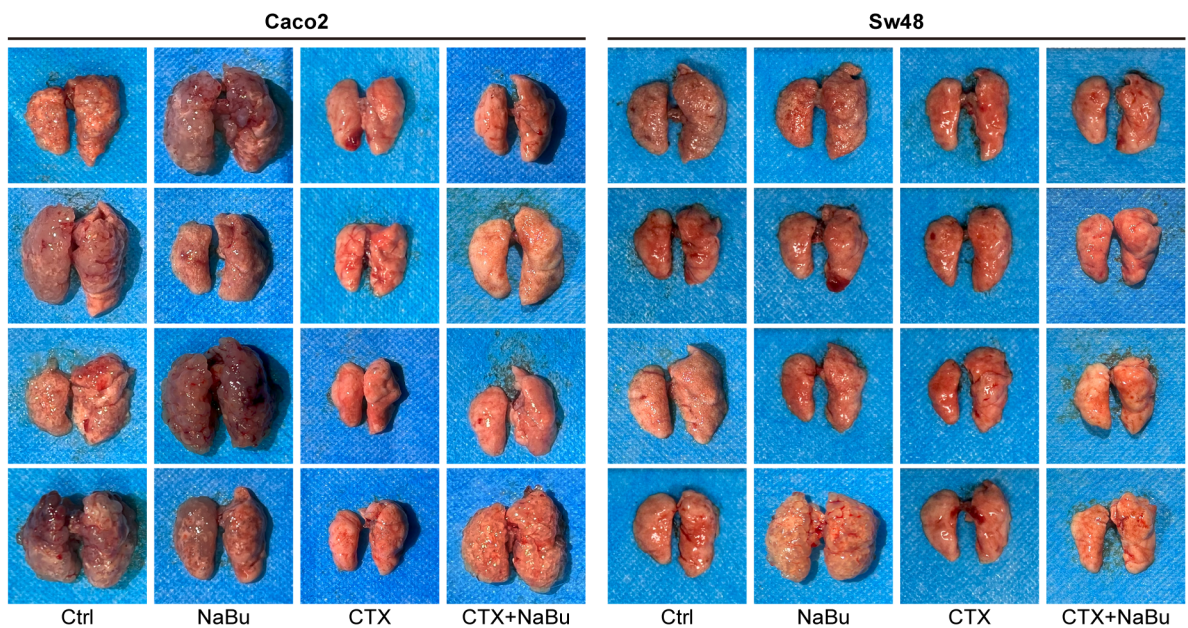


Figure S3. Supplementary in vivo analyses of subcutaneous xenograft and pulmonary metastasis models. (A) Tumor volumes of Caco2 and Sw48 xenografts were measured at the indicated time points after tumor inoculation and are shown as growth curves. CTX was initiated on day 15. Longitudinal comparisons were performed using a mixed-effects model accounting for repeated measurements within mice. Representative photographs of mice bearing subcutaneous xenografts (Caco2 and Sw48) under the indicated treatments (Ctrl, NaBu, CTX, CTX+NaBu) at the experimental endpoint, prior to tumor excision, are shown for visual reference. (B) Pulmonary metastasis model: lungs from the remaining animals (4 per group) are shown here. Representative images of one mouse per group are presented in Figure 6C. Statistical significance: ns, not significant; *** $p < 0.0001$.

Supplementary Figure 4:

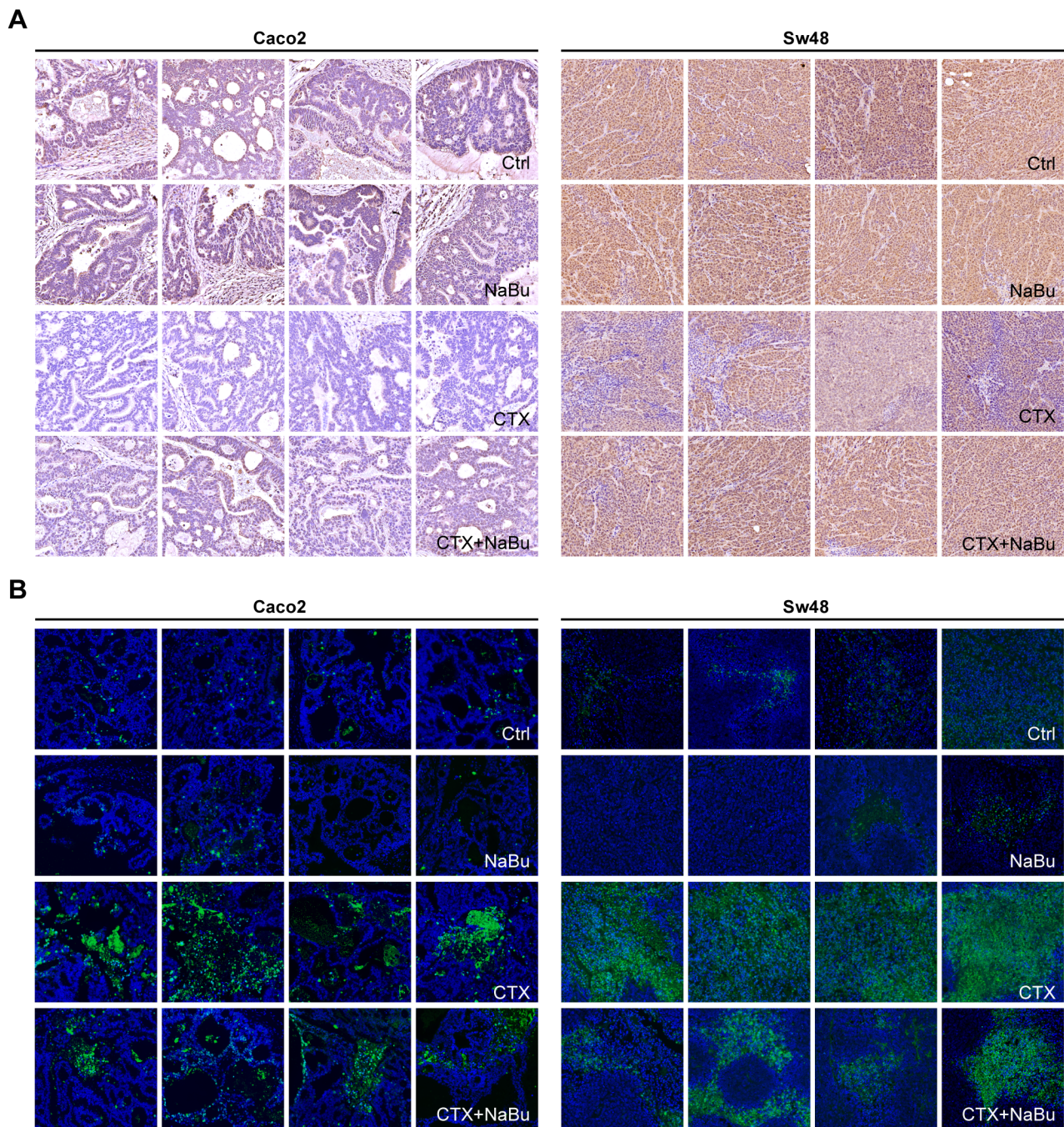


Figure S4. Ki67 and TUNEL staining of subcutaneous tumors (additional samples). (A) Ki67 staining in Caco2 and SW48 xenografts under the indicated treatments (Ctrl, NaBu, CTX, CTX+NaBu). (B) TUNEL staining of tumor sections from the same animals. Representative images from one mouse per group are shown in Figure 7A; the remaining four mice per group are displayed here to provide complete experimental data.

Supplementary Figure 5:

A

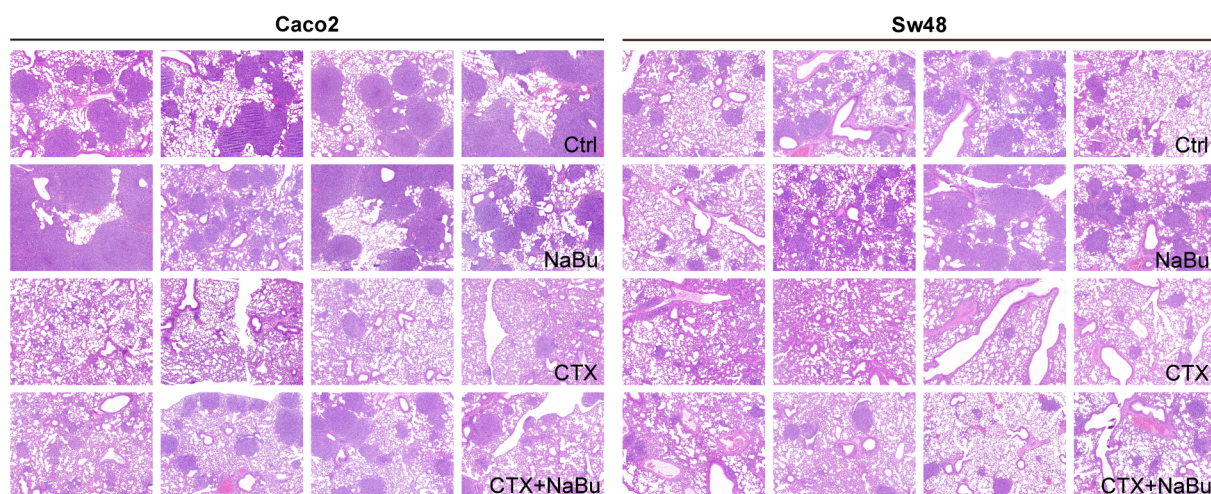


Figure S5. H&E staining of lung sections from pulmonary metastasis models (additional samples). (A) H&E staining in Caco2 and SW48 pulmonary metastasis models under the indicated treatments (Ctrl, NaBu, CTX, and CTX + NaBu). Representative images from one mouse per group are shown in Figure 7B; the remaining animals are presented here to provide the complete experimental dataset.

Supplementary Figure 6:

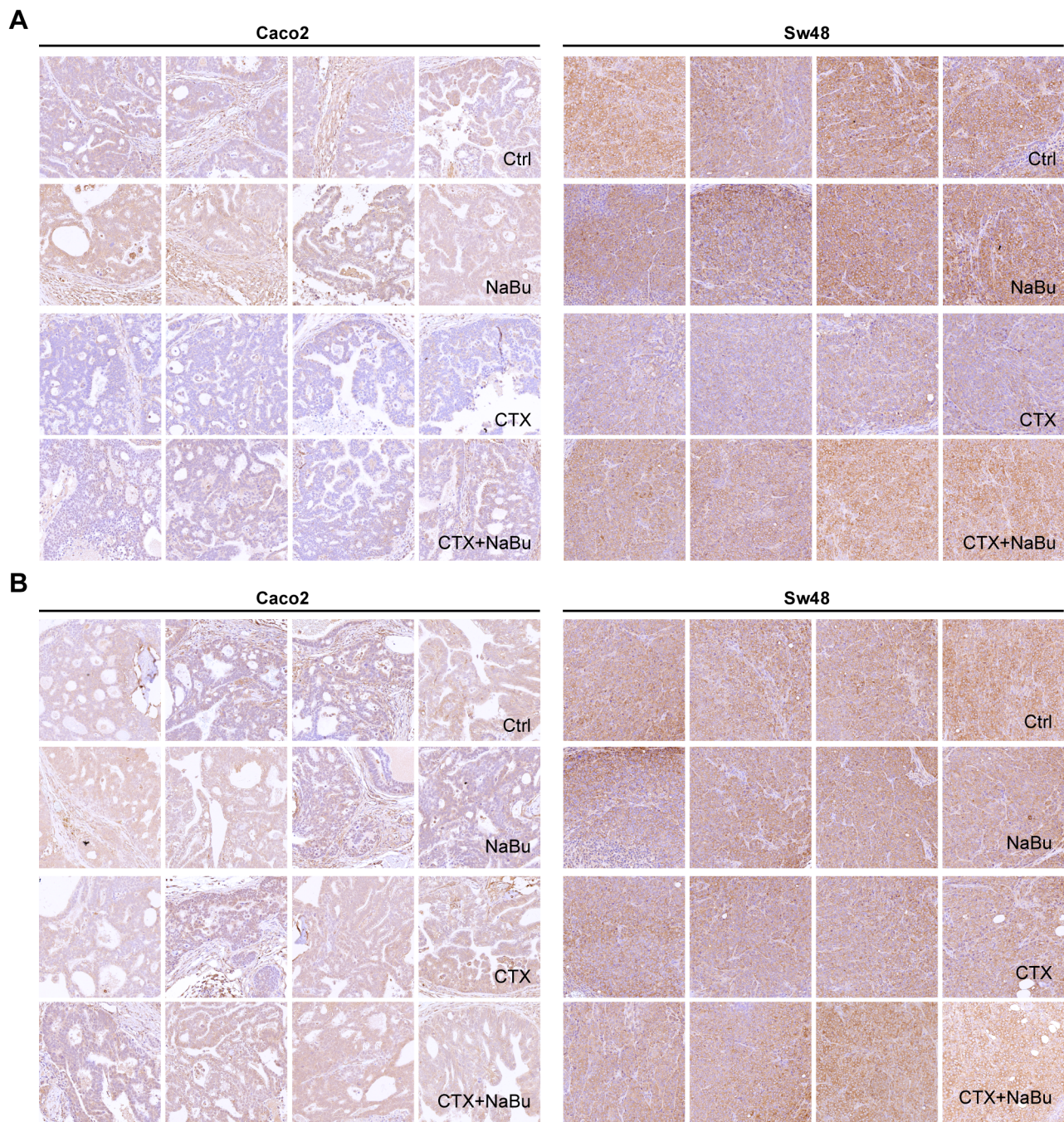


Figure S6. Immunohistochemistry of p-EGFR and EGFR in subcutaneous tumors (additional samples). (A) p-EGFR and (B) EGFR staining in Caco2 and SW48 xenografts under the indicated treatments (Ctrl, NaBu, CTX, and CTX + NaBu). Representative images from one mouse per group are shown in Figure 7C; the remaining animals are presented here to provide the complete experimental dataset.

Supplementary Figure 7:

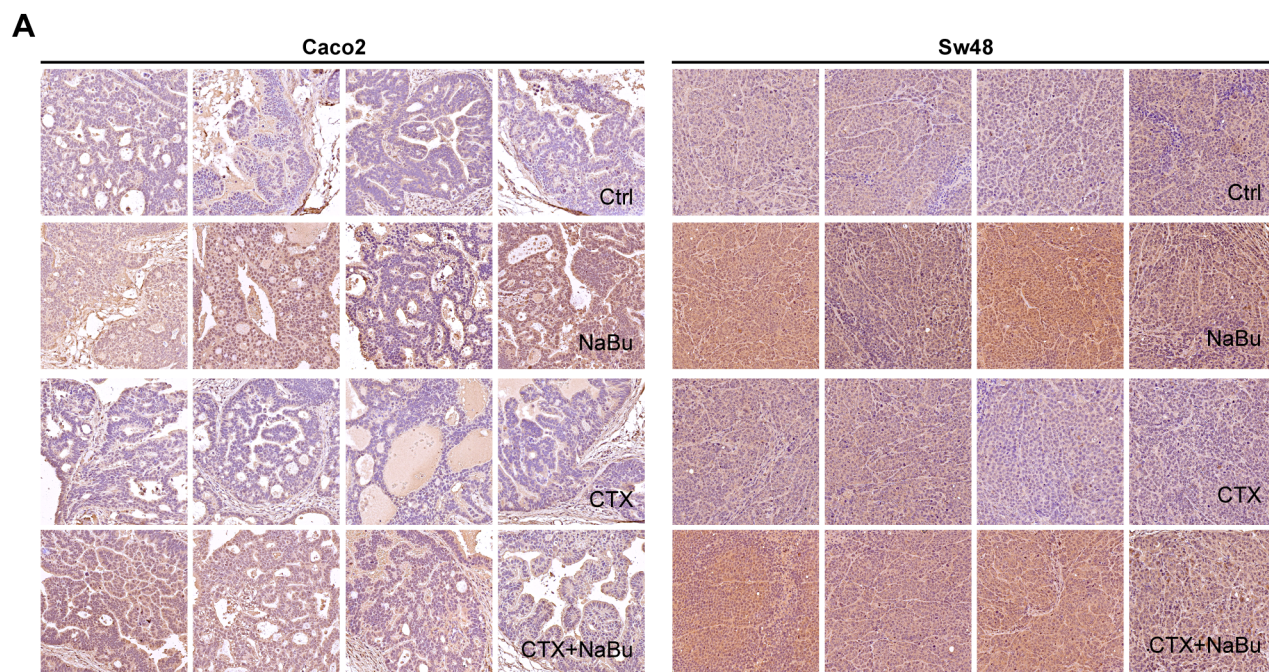


Figure S7. Immunohistochemistry of Wip1 in subcutaneous tumors (additional samples). (A) Wip1 staining in Caco2 and SW48 xenografts under the indicated treatments (Ctrl, NaBu, CTX, and CTX + NaBu). Representative images from one mouse per group are shown in Figure 7C; the remaining animals are presented here to provide the complete experimental dataset.

Supplementary Table 1: Primary and secondary antibodies used in this study.

Target Protein	Species	Dilution		Supplier	Catalog No.
		WB	IHC		
p-EGFR (Tyr1068)	Rabbit	1:1000	1:100	CST	#3777
EGFR	Rabbit	1:1000	1:100	Abcam	ab32077
WIP1	Mouse	1:5000	1:200	Proteintech	67440-1-Ig
p-AMPK α (Thr172)	Rabbit	1:1000	—	Beyotime	AF5908
AMPK α 1/2	Rabbit	1:1000	—	Beyotime	AF6195
p-Akt (Ser473)	Rabbit	1:1000	—	CST	#4060
Akt (pan)	Rabbit	1:1000	—	CST	#4691
p-p53 (Ser392)	Rabbit	1:1000	—	Boster	BM4095
P53	Rabbit	1:1000	—	Boster	PB9008
p-Erk1/2 (Thr202/Tyr204)	Rabbit	1:1000	—	CST	#4370
Erk1/2	Rabbit	1:1000	—	CST	#4695
MEK1/2	Rabbit	1:1000	—	Abcam	ab178876
p-p38 (Thr180/Tyr182)	Rabbit	1:1000	—	Proteintech	28796-1-AP
p38	Rabbit	1:1000	—	Boster	BM4439
P21	Rabbit	1:1000	—	Proteintech	10355-1-AP
Ki67	Rabbit	—	1:1000	Proteintech	28074-1-AP
β -Actin	Mouse	1:5000	—	Proteintech	66009-1-Ig
Goat anti-Rabbit IgG (HRP, recomb.)	Goat	1:5000	—	Proteintech	RGAR001
Goat anti-Mouse IgG (HRP, recomb.)	Goat	1:5000	—	Proteintech	RGAM001